論文 / 著書情報
Article / Book Information

Title	Magnetron Sputtering Preserves Solid Electrolyte Toughness after Shot Peening and Enhances Critical Current Density in Lithium-Metal Anode All-Solid-State Batteries
Authors	Atsuro OKUMURA, Hito FUKUSUMI, Manabu KODAMA
Citation	Electrochemistry, Vol. 93, No. 9, p. 097001
Pub. date	2025, 8
DOI	https://doi.org/10.5796/electrochemistry.25-00094
Creative Commons	Information is in the article.

Electrochemistry
The Electrochemical Society of Japan
Received: June 1, 2025
Accepted: July 25, 2025
Published online: August 1, 2025
Issued: September 6, 2025
https://doi.org/10.5796/electrochemistry.25-00094
Article
Electrochemistry, **93(9)**, 097001 (2025)

Magnetron Sputtering Preserves Solid Electrolyte Toughness after Shot Peening and Enhances Critical Current Density in Lithium-Metal Anode All-Solid-State Batteries

OPEN ACCESS

Atsuro OKUMURA, Hito FUKUSUMI, and Manabu KODAMA*,§

Department of Mechanical Engineering, School of Engineering, Institute of Science Tokyo, 2-12-1 Ookayama, Meguro-ku, Tokyo 152-8550, Japan

* *Corresponding author: kodama.m.d0f2@m.isct.ac.jp*

ABSTRACT

To enable fast charging in lithium-metal anode all-solid-state batteries, the suppression of lithium dendrite formation at the solid electrolyte (SE) interface is critical. Gold (Au) sputtering has been proposed to enhance interfacial contact and mitigate dendrite growth; however, conventional sputtering can thermally damage the SE and degrade its fracture toughness. In this study, we investigated magnetron sputtering as a low-damage deposition technique for applying Au interlayers. The magnetically confined plasma in magnetron sputtering minimizes the surface exposure and thermal degradation of the SE, potentially preserving its mechanical integrity. Lithium garnet-type SEs with and without shot peening (SP) were prepared and coated with Au via normal and magnetron sputtering. Critical current density (CCD) and fracture toughness were evaluated for each condition. Without SP, CCD improvement was limited and independent of the sputtering method. In contrast, with SP, CCD was significantly enhanced, and magnetron sputtering yielded a higher CCD than normal sputtering. Fracture toughness measurements revealed that thermal damage from normal sputtering reduced toughness, whereas magnetron sputtering preserved it. These results demonstrate that combining SP with magnetron sputtering effectively improves the SE interfacial properties, thereby enhancing the fast-charging capability.

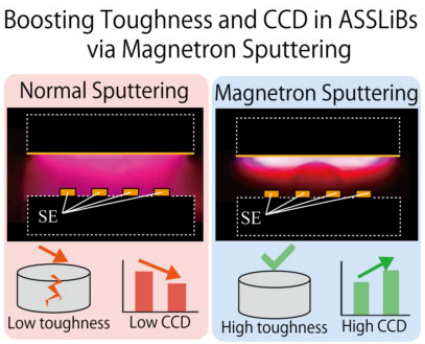

Keywords : All-solid-state Battery, Oxide Solid Electrolyte, Magnetron Sputtering, Fast Charging

1. Introduction

To promote carbon neutrality, the development of safer and higher-capacity batteries for electric vehicles is essential. Conventional lithium-ion batteries rely on organic liquid electrolytes, which pose a risk of ignition. As a promising alternative, all-solid-state lithium-ion batteries (ASSLiBs) employ flame-retardant inorganic solid electrolytes (SEs), offering improved safety. Furthermore, the use of lithium-metal anodes in ASSLiBs can significantly enhance energy density because the theoretical capacity of lithium metal is nearly 10 times greater than that of graphite.[1,2] However, under high-rate charging conditions, lithium dendrites tend to form within the SE, leading to internal short circuits and limiting the critical current density (CCD).[3] Therefore, strategies to suppress dendrite growth and enhance interfacial properties are crucial for realizing fast-charging ASSLiBs.

Notably, rapid charging can be achieved by improving the CCD (i.e., the current density at which an internal short circuit occurs). Lithium dendrites typically grow from the non-uniform lithium deposition caused by electrochemical contact defects at the anode interface during charging. Electrochemical contact defects involve anode interface delamination, which occurs when lithium diffusion is insufficient during the lithium dissolution process under discharge conditions.[4] Therefore, maintaining good electrochemical contact at the interface between the lithium-metal anode and SE is considered effective in suppressing lithium dendrite growth during charging. For example, a metal intermediate layer can simply be inserted at the interface. Temporary alloying of the interlayer with lithium improves the interfacial contact and promotes uniformity of the interfacial reaction.[5] Sputtering is often employed to deposit metals owing to the high purity and uniformity of the resulting thin films. During this process, the metal is deposited by hitting the source target with cations, which are produced by converting a gas into a plasma by high-voltage discharge, to repel the constituent atoms of the target metal.[6] Shot peening (SP) is also effective in suppressing lithium dendrites because it increases the fracture toughness of the oxide SE surface. Fracture toughness is an important property that characterizes a material's brittleness or resistance to fracture.[7] Given that lithium dendrites grow as cracks propagate within the SE, increasing the fracture toughness of the SE surface is effective in suppressing the growth of lithium dendrites. It has been shown that Au sputtering after SP on the SE surface improves the CCD compared with either process alone, and the charging rate is approximately 20 times faster with Au and SP than that without SP.[8] However, further improvement of the CCD is required to significantly reduce the charging time in electric vehicles. Previously, normal sputtering was used to deposit an Au layer at the interface between the SE and the lithium-metal anode; the generated plasma is shown in Fig. 1a. Plasma is expected to cause thermal damage to the SE surface during sputtering, causing a decrease in the SE fracture toughness.[8] If sputtering can be performed without causing thermal damage to the SE, the reduction in fracture toughness and growth of lithium dendrites may be

§ECSJ Active Member
M. Kodama orcid.org/0000-0002-6870-2450

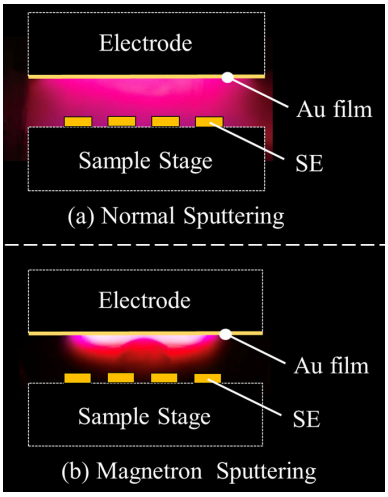

Figure 1. Plasma distribution obtained during (a) normal sputtering and (b) magnetron sputtering.

reduced, potentially leading to a higher CCD. Therefore, magnetron sputtering was considered in the present study. The plasma generated during magnetron sputtering is shown in Fig. 1b; magnetic pressure is generated by a magnet mounted inside the top electrode, and the plasma is dense only near the target metal.[9] Hence, only a dilute plasma exists near the SE surface, which may reduce the thermal damage and support high CCDs.

In this study, the effect of Au deposition by magnetron sputtering on the fracture toughness of the SE was investigated, and the correlation with CCD was examined to determine the improvement in the charging performance of oxide-based lithium-metal anode ASSLiBs. Specifically, Au layers were deposited on SEs with and without SP processing by normal sputtering and magnetron sputtering, and CCD tests and fracture toughness measurements were performed.

2. Experimental

2.1 Material synthesis

A Ga-doped garnet-type oxide, namely $Li_{6.25}Ga_{0.25}La_3Zr_2O_{12}$ (LGLZO), was used as the SE. Ga doping was found to be promising because the desirable cubic phase and a dense microstructure can be readily obtained.[10] The synthesis of LGLZO is described as follows. The starting materials, La_2O_3 (99.9 %, Kojyundo Chemicals), ZrO_2 (98 %, Kojyundo Chemicals), Ga_2O_3 (99.99 %, Wako Chemicals), and LiOH (98 %, Alfa Aesar), were weighed in a prescribed amount, placed in a magnetic agate mortar, and stirred at 100 rpm for 5 min. Then, 18 g of the mixed material was divided into two zirconia pots (50 mL, Ito Seisakusho), and 20 zirconia balls (Φ10 mm × 10 mm, Φ5 mm × 10 mm) and 30 mL of hexane (95 %, Hayashi Pure Chemical) were placed in each pot. The mixtures were processed at 300 rpm for 2 h. After ball milling, the materials were dried on a hot plate and in a vacuum drying oven, and then placed in a platinum crucible (25 ml, Tanaka Kikinzoku Kogyo) and calcined in an electric furnace (CWF13/5, CARBOLITE GERO) at 800 °C for 12 h (temperature increase rate: 5 °C/min, decrease rate: 2 °C/min). After calcination, the hardened material was ground using a stainless-steel mortar and pestle, and the resulting powder was ball milled and dried under the same conditions. The powder was then pressed into 5 mm diameter pellets at 150 MPa using a hydraulic press (TB-20H, Sansho Industries). The pellets and mother powder (powder sieved to a fine grain size before molding) were placed in layers in a platinum crucible and fired in an electric furnace at 1050 °C for 12 h (temperature increase rate: 5 °C/min, decrease rate: 2 °C/min). Pellets were formed from the calcined mass using a leutor, and the pellet surfaces were smoothed with 1500 grit sandpaper in the air to obtain LGLZO disks with diameters of 4 mm and thicknesses of 1 mm.

2.2 Shot peening on solid electrolyte surface

In the SP process, media is blown by compressed air from a compressor (MCP-25SLMA, Monotaro) against both sides of the SE pellets in the air. Al_2O_3 powder (50 µm diameter) with an angular shape was used as the media. The compressed air pressure was 0.4 MPa, the distance from the SP gun to the SE pellet was 10 cm, and the processing time was 10 s. After SP processing, the SE surface was sprayed with compressed air without media to remove any residual media.

2.3 Au film formation on SE surfaces by sputtering

Au thin films (~200 nm thick) were deposited on the SE pellet surfaces by normal sputtering (SC-701Mk II DC, Sanyu Electron) and magnetron sputtering (SC-701HMC, Sanyu Electron). Although different devices were used, the electrode size and distance between electrodes were generally the same, and the only difference between the two devices was the application of a magnetic field. The ultra-small-angle X-ray scattering system was used to measure the deposition rate of Au thin films deposited by normal and magnetron sputtering. The deposition rate of Au thin films was calculated for each sputtering system based on the difference in X-ray transmission intensity between an untreated Kapton tape and a Kapton tape that was sputtered for 10 min. The deposition rate of normal sputtering is 14.03 nm/min, and that of magnetron sputtering is 30.33 nm/min. Based on these data, Au thin films of about 200 nm were deposited on the surface of the SE. During sputtering, the edges of the pellet top surfaces were covered to prevent Au adhering to the sides of the pellets, which can cause short circuits in the fabricated cells. This was achieved by masking the pellets using a plate with 5-mm-diameter holes and Cu tape with 3.2-mm-diameter holes. In both systems, sputtering was performed by drawing a vacuum in the chamber and then supplying argon gas. After sufficient vacuuming, the ion current was kept constant by adjusting the argon gas supply rate to maintain a uniform environment inside the chamber. Based on the calculated deposition rate, the sputtering time was determined, and the thickness of the Au film formed on the SE surface was kept constant. Normal sputtering was performed for 16 min and magnetron sputtering for 7 min 24 s.

2.4 Measurement of the CCD

Lithium symmetric cells were fabricated using SEs with each surface treatment, and the charging performance was measured.[11] First, 4 mm diameter Li foils were attached to both sides of SE pellets in an argon-filled glove box filled with a low dew point, considering the reactivity of Li with nitrogen and oxygen. The lithium symmetric cell was pressurized using a spring, and 5 MPa was always applied by adjusting the deflection of the spring with a screw tightener. The lithium symmetric cell was sealed in an argon-filled airtight container with a molecular sieve as a moisture absorbent, considering that the current-carrying test was conducted outside the glove box. The CCD test is an endurance test in which the current density is increased with each cycle, and the cell is energized until it finally shorts out. The higher the current density at the time of short circuit, the more the growth of lithium dendrites has been suppressed. When lithium is stably deposited, the voltage proportionally increases as the current density is gradually increased. Conversely, when a cell is short-circuited owing to lithium dendrite growth, a distinct voltage drop is observed. In this study, CCD measurements were conducted using a charge-discharge tester (EF-7100P, Electrofield), and the cells were placed in a thermostatic chamber (SU-241, ESPEC Corp.) set at 60 °C during testing. The

test was started 2 h after the cells were placed in the chamber to stabilize the cell temperature before evaluating the charging performance.

2.5 Measurement of the fracture toughness

The fracture toughness of the SE surface was measured by indentation using a Vickers hardness tester (HM-201C, Mitutoyo), and the surface was observed by scanning electron microscopy (TM-4000, Hitachi High-Tech). The fracture toughness can be calculated from the lengths of the indentation marks and the cracks extending from the four corners of the indentation marks using Eq. 1,[12] where K_c is the fracture toughness [Pa-m1/2], E is the Young's modulus [Pa], P is the indenter load [N], and a and c are the average indentation diagonal half-length [m] and the average crack half-length [m], respectively. The Young's modulus reported for LLZO (130 GPa) was used.[13] The indenter load was 1 kgf.

$$K_c = 0.026 \frac{E^{\frac{1}{2}} P^{\frac{1}{2}} a}{c^{\frac{3}{2}}} \quad (1)$$

3. Results and Discussion

To evaluate the effect of magnetron sputtering on cell charging performance, CCD testing and fracture toughness measurements were performed on SEs with six different surface preparation processes. Figure 2 illustrates the processes applied to each of the six samples. Sample A was only smoothed using sandpaper. Sample B underwent SP after surface smoothing with sandpaper. Sample C was coated with a 200 nm Au film by normal sputtering after surface smoothing using sandpaper. Sample D was coated with a 200 nm Au film by magnetron sputtering after surface smoothing using sandpaper. Sample E was smoothed using sandpaper, followed by SP, and then coated with a 200 nm Au film by normal sputtering. Sample F was smoothed using sandpaper, followed by SP, and then coated with a 200 nm Au film by magnetron sputtering. The SE is stored in a glove box in the argon atmosphere but is removed when each process is performed. It is exposed to the air for about 10 min when only surface smoothing is performed and for about 30 min when both surface smoothing and SP are performed. Because the sputtering environment is the argon atmosphere, it is not included in the atmospheric exposure time. After each process, the SE is immediately moved to a glove box.

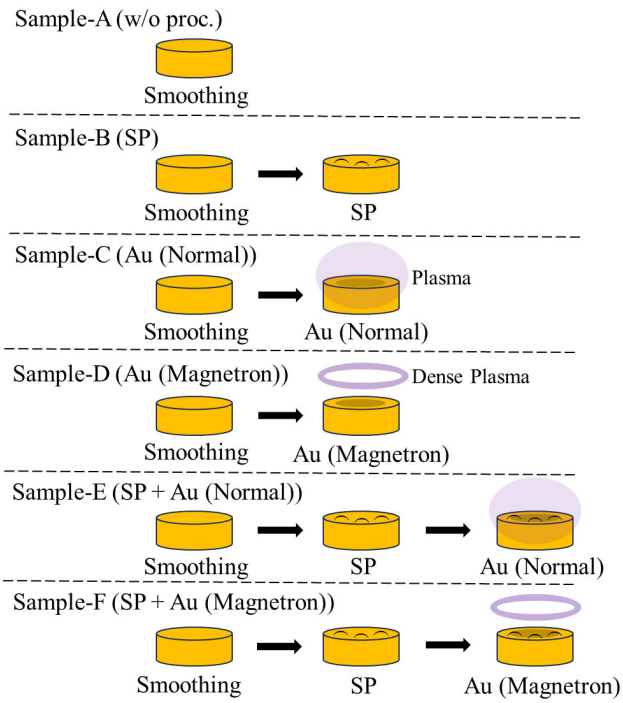

Figure 2. Illustration of the six processes employed for preparing the SE pellet samples.

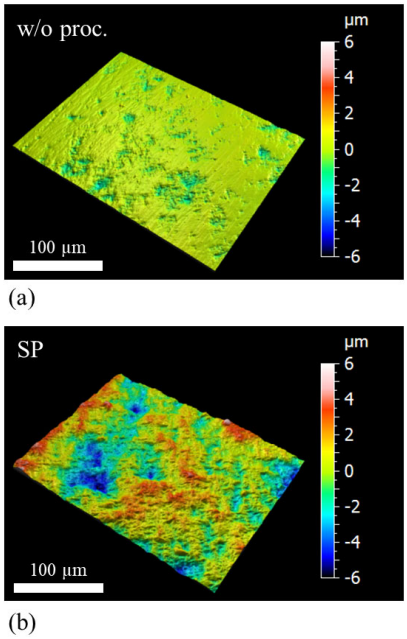

Figure 3. Surface 3D SEM images of (a) the sample without processing and (b) the sample treated with SP.

Figure 3 shows the 3D SEM images of the surface of Sample A and Sample B. In the case of non-processed sample (Sample A), as shown in (a), a slight indentation made by smoothing with sandpaper can be seen on the surface. In the case of sample underwent SP (Sample B), the surface is uneven as shown in (b), with the square roughness of 1.05 μm. A previous study conducted under the same conditions found that the increase in surface area due to the unevenness formed on the SE surface by SP was less than 10 %. This unevenness was not significant enough to cause power concentration.[8] It is necessary to confirm whether the Al_2O_3 powder used as a medium during SP forms a layer on the SE surface. A previous study in which SP was performed under the same conditions confirmed the absence of an Al_2O_3 layer on the SE surface using the Auger spectroscopy.[8] Therefore, the alumina particles used for SP do not affect the charge-discharge test.

3.1 CCD results for each condition

The polarization curves obtained from the CCD tests under each condition are shown in Fig. 4. For all surface treatment conditions, a distinct voltage drop was observed at a certain current density, when lithium dendrites reached the positive electrode. The transport resistance of electrons in the lithium dendrite is much smaller than the transport resistance of lithium ions in the SE. Therefore, the impedance of the cell suddenly drops during a short circuit, causing a sudden drop in the cell voltage.[14]

The CCD without SP is shown in Fig. 5a, presented for the three conditions: no sputtering, normal sputtering, and magnetron sputtering. The CCD was improved by Au deposition, but the CCD was approximately 0.2 mA/cm^2 for both sputtering methods, and no significant difference was observed. The CCD with SP is shown in Fig. 5b, also presented for the three conditions: no sputtering, normal sputtering, and magnetron sputtering. The CCD was further improved by each sputtering method after SP, but the CCD was more significantly improved by magnetron sputtering. With SP, the CCD was ~0.93 mA/cm^2 with normal sputtering and

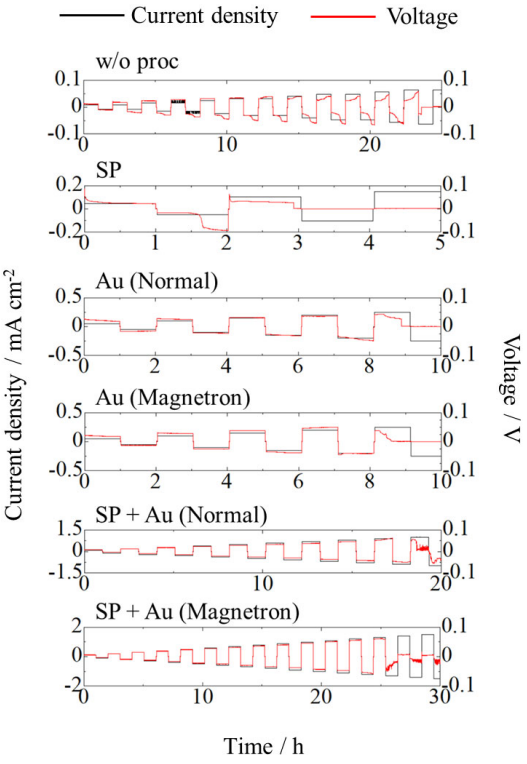

Figure 4. Polarization curves of the six tested samples.

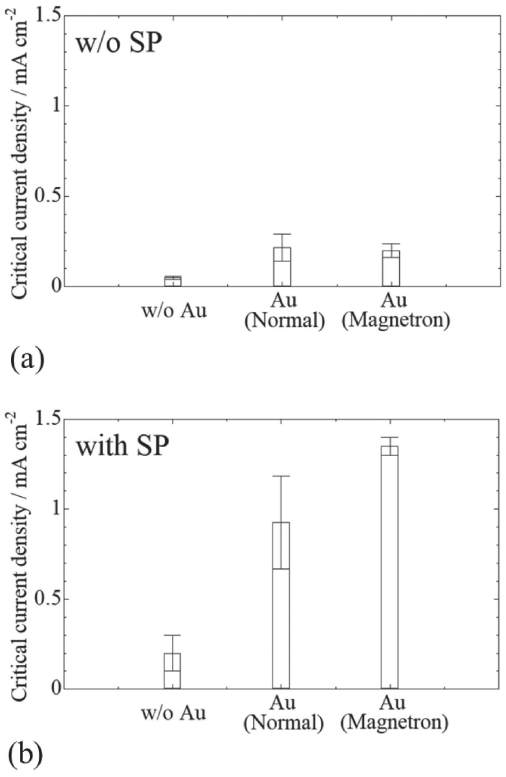

Figure 5. The CCD obtained (a) without SP and (b) with SP.

$\sim$1.35 mA/cm^2 with magnetron sputtering, showing a significant improvement in charging performance.

Without sputtering, the CCD is approximately 4 times higher with SP than without SP. Thus, changes in the mechanical properties of the SE due to SP affect the CCD. Although the CCD does not change significantly for the different sputtering methods without SP,

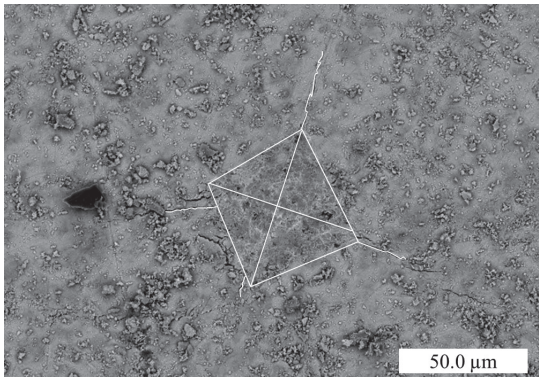

Figure 6. Image of the crack and the indentation on the SE surface.

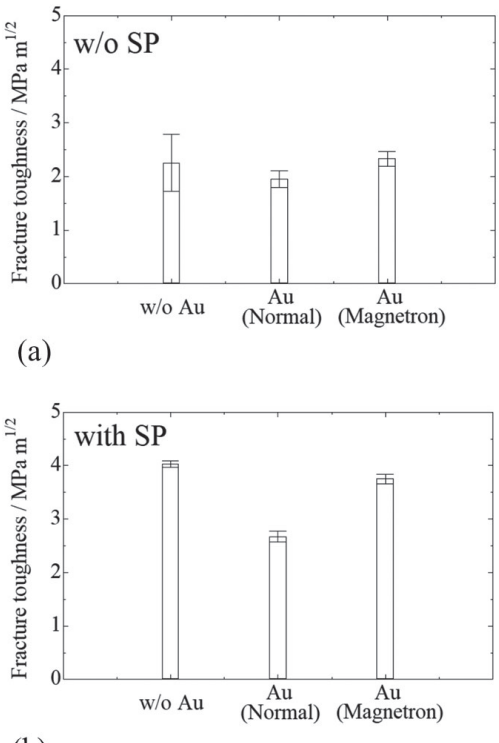

Figure 7. Fracture toughness of the SE surfaces (a) without SP and (b) with SP.

with SP, the CCD is significantly improved after Au deposition by magnetron sputtering. Therefore, we measured the fracture toughness of SE under each surface processing condition and compared the findings with the CCD results.

3.2 Fracture toughness results for each condition

To observe the mechanical strength on the SE surface, the fracture toughness was measured with the indentation system. Figure 6 shows the crack and the indentation on the SE surface with Au thin film applied using the Vickers hardness tester. The fracture toughness measurements ($n = 6$) were made under various conditions based on the dimensions of the indentation and cracks imaged using the 3D SEM, and the results are compared below.

The fracture toughness of the SE surfaces without SP is shown in Fig. 7a, presented for the three conditions: no sputtering, normal sputtering, and magnetron sputtering. No significant differences in fracture toughness were observed among the three conditions.

Without SP, the original fracture toughness was low, and the sputtering method had little effect on the fracture toughness. This is thought to be the reason why there is no difference in the CCD between the different sputtering methods, without SP (Fig. 5a). The fracture toughness of the SE surfaces with SP is shown in Fig. 7b, also presented for the three conditions: no sputtering, normal sputtering, and magnetron sputtering. Normal sputtering significantly decreased the fracture toughness that had been improved by SP. This may be due to the thermal damage caused by the contact of the plasma with the SE surface during normal sputtering. Notably, a slight decrease in fracture toughness can also be observed when magnetron sputtering is used. As mentioned above, magnetron sputtering induces a dense plasma near the electrodes because of magnetic pressure, and a dilute plasma also exists near the SE surface. The significant reduction in fracture toughness observed with SP is assumed to be due to the increased fracture toughness being canceled out by the high thermal damage caused by the plasma. Conversely, the slight decrease in fracture toughness without SP is assumed to be because there is no increase in fracture toughness on the SE surface. Therefore, there is little factor reducing fracture toughness due to high thermal damage. This may explain why the reduction in fracture toughness due to spatter is usually larger when SP is performed.

The dilute plasma may have slightly reduced the fracture toughness, but the CCD was still significantly improved, even compared with normal sputtering (Fig. 5b). Therefore, the insertion of an Au interlayer by low-damage magnetron sputtering is effective in improving charging performance.

Thus, SP increases fracture toughness of the SE surface and thus improves the mechanical property of the SE. However, as mentioned above, SP does not affect the electrochemical properties of SE. It is quite possible that surface smoothing and SP in the air may form the inactive surface layer. It has been reported that the inert layer on the SE surface can be removed by using a short acid etching procedure (e.g., HCl).[15] It is possible to further improve the CCD by adding a short acid etching procedure and magnetron sputtering after surface smoothing using sandpaper and SP. The authors would like to set it as our future work.

4. Conclusions

We attempted to enhance the charging performance of lithium-metal anode ASSLiBs by employing an alternative Au sputtering method. Specifically, magnetron sputtering and normal sputtering were applied to SEs with and without SP, followed by CCD testing and fracture toughness measurements. Magnetron sputtering enables the deposition of an Au layer on the SE with minimal damage, owing to the dense arrangement of sputtered atoms near the target metal under magnetic confinement. Applying the Au film suppresses the growth of lithium dendrites, and magnetron sputtering maintains the mechanical integrity of the SE layer, further suppressing the dendrite formation and growth. Without SP processing, the improvement in CCD by Au sputtering was limited, and no significant differences were observed between the sputtering methods. The fracture toughness was also similar across all conditions, suggesting that the low intrinsic toughness of the original specimens was not significantly degraded by either sputtering technique. In contrast, magnetron sputtering significantly improved the CCD while preserving the enhanced fracture toughness induced by SP, whereas normal sputtering reversed the effects of SP. These results indicate that low-damage Au layer deposition via magnetron sputtering promotes the enhancement of CCD while minimizing the degradation in fracture toughness. Ultimately, the combination of SP processing and magnetron sputtering is effective for further improving the performance of lithium-metal anode ASSLiBs.

Acknowledgments

This study was supported by the Japan Keirin Autorace Foundation.

CRediT Authorship Contribution Statement

Atsuro Okumura: Investigation (Lead), Methodology (Lead), Resources (Lead), Writing – original draft (Lead)
Hito Fukusumi: Investigation (Equal), Methodology (Equal), Resources (Equal)
Manabu Kodama: Conceptualization (Lead), Supervision (Lead), Writing – review & editing (Lead)

Conflict of Interest

The authors declare no conflict of interest in the manuscript.

Funding

JKA Foundation

References

1. J. Wang, Q. Zheng, M. Fang, S. Ko, Y. Yamada, and A. Yamada, *Adv. Sci.*, **8**, 2101646 (2021).
2. X. Zhang and C. Sun, *Chem. Lett.*, **51**, 891 (2022).
3. B. Wu, S. Wang, J. Lochala, D. Desrochers, B. Liu, W. Zhang, J. Yang, and J. Xiao, *Energy Environ. Sci.*, **11**, 1803 (2018).
4. T. Krauskopf, H. Hartmann, W. G. Zeier, and J. Janek, *ACS Appl. Mater. Interfaces*, **11**, 14463 (2019).
5. J. Wakasugi, H. Munakata, and K. Kanamura, *J. Electrochem. Soc.*, **164**, A1022 (2017).
6. R. Garg, S. Gonuguntla, S. Sk, M. S. Iqbal, A. O. Dada, U. Pal, and M. Ahmadipour, *Adv. Colloid Interface Sci.*, **330**, 103203 (2024).
7. G. D. Quinn, *Mechanical Properties and Performance of Engineering Ceramic Engineering Ceramics II: Ceramic Engineering and Science Proceedings*, Vol. 27, Chapter 5 (2006).
8. M. Kodama, K. Takashima, and S. Hirai, *J. Power Sources*, **537**, 231556 (2022).
9. P. J. Kelly and R. D. Arnell, *Vacuum*, **56**, 159 (2000).
10. M. Mishra, C. W. Hsu, P. C. Rath, J. Patra, H. Z. Lai, T. L. Chang, C. Y. Wang, T. Y. Wu, T. C. Lee, and J. K. Chang, *Electrochim. Acta*, **353**, 136536 (2020).
11. M. Klimpel, H. Zhang, M. V. Kovalenko, and K. V. Kravchyk, *Commun. Chem.*, **6**, 192 (2023).
12. C. B. Ponton and R. D. Rawlings, *Mater. Sci. Technol.*, **5**, 865 (1989).
13. J. E. Ni, E. D. Case, J. S. Sakamoto, E. Rangasamy, and J. B. Wolfenstine, *J. Mater. Sci.*, **47**, 7978 (2012).
14. M. Siniscalchi, Y. Shi, G. Li, J. S. Gibson, R. S. Weatherup, R. S. Bonilla, S. C. Speller, and C. R. M. Grovenor, *Energy Environ. Sci.*, **17**, 2431 (2024).
15. M. Motoyama, Y. Tanaka, T. Yamamoto, N. Tsuchimine, S. Kobayashi, and Y. Iriyama, *ACS Appl. Energy Mater.*, **2**, 6720 (2019).